Structure identification based on steady-state control: Experimental results and applications

Mattia Frasca,[1,2,*] Dongchuan Yu,[3,†] and Luigi Fortuna[1,2,‡]

[1]*Dipartimento di Ingegneria Elettrica, Elettronica e dei Sistemi, Università degli Studi di Catania, viale A. Doria 6, 95125 Catania, Italy*

[2]*Laboratorio sui Sistemi Complessi, Scuola Superiore di Catania, Via San Nullo 5/i, 95123 Catania, Italy*

[3]*School of Automation Engineering, University of Electronic Science and Technology of China, Chengdu 610054, China*

(Received 3 June 2009; revised manuscript received 8 October 2009; published 24 February 2010)

We report experimental results on structure identification of nonlinear systems by a steady-state control method. The idea underlying the method is to drive the nonlinear system to steady state by applying a suitable feedback control input. It turns out experimentally that this control-based structure identification method can be used for some applications, such as estimation of initial conditions and state variables of nonlinear systems and structure identification of some special elements. Two attractors of the Chua oscillator are presented to illustrate the reliability of the suggested techniques under the hypotheses of measurable state variables and physical access to the system for implementing the proportional feedback.

DOI: 10.1103/PhysRevE.81.026212 PACS number(s): 05.45.Xt

I. INTRODUCTION

Mathematical models can be used to quantitatively understand dynamical behavior of natural or artificial systems. In some cases, the structure of these mathematical models can be derived from first principles and only some model parameters have to be determined from experimental data. This problem has been well studied in the literature and recently has regained considerable interest especially for chaotic systems. Several methods have been suggested based on autosynchronization [1–12] (such methods derive from the basilar concept of synchronization in chaos theory [13–15]), balanced synchronization [16,17], partial synchronization [18,19], parametric optimization [20–23], nonlinear filters [22,24], or special properties of the feedback structure in systems with delayed feedback [25]. The problem of parameter estimation in time-delay systems has been recently addressed with specific techniques [26,27]. In particular, in [26] to estimate the delay time the idea of disturbing the system by a short-correlated noisy signal of large amplitude is exploited, and the delay is then identified by analyzing the correlation function, while in [27] it is the analysis of the system response to regular external impulsive perturbations that allows the reconstruction of the time-delay system parameters.

However, many parameter estimation methods are applicable under the assumption that the structure of these mathematical models is known accurately and their performance may dramatically be deteriorated even in the presence of small structure error. In practice, however, the structure of the mathematical models usually is not or only partially known. Therefore, to understand the dynamical behavior of systems of interest, one first has to identify the system structure. Such an issue has not been fully investigated especially for complex dynamical systems.

Recently, the use of control-based methods for estimating the structure of complex systems has been investigated in several works [28–32]. The idea underlying the method is to drive the system to steady states by adding to the system suitable feedback control inputs. The method has been successfully applied to the identification of the system dynamics [28], to estimate the topology of a complex network [29,30], and to identify the delays underlying a nonlinear dynamical system [31,32]. In this article, we report experimental structure identification of chaotic circuits using the control-based method and show that the control-based structure identification method can be applied to some applications of physical interest, such as system modeling and structure identification of some special elements.

To illustrate the reliability of the suggested techniques, we consider a Chua oscillator described by the following dimensionless equations [33]:

$$\dot{x}_1 = \delta\alpha[x_2 - h(x_1)],$$

$$\dot{x}_2 = \delta(x_1 - x_2 + x_3),$$

$$\dot{x}_3 = \delta(-\beta x_2 - \gamma x_3), \tag{1}$$

with $h(x)=m_1x+0.5(m_0-m_1)(|x+1|-|x-1|)$. The Chua oscillator is a well-known generalization of the Chua's circuit, in the sense that it can implement all the dynamics of the Chua's circuit [34,35] and, moreover, every dynamics that can be generated by any member of the Chua's family can be obtained in the Chua oscillator. So, quoting Chua [36], this circuit represents "structurally the simplest and dynamically the most complex member of the Chua's circuit family."

In this paper, two chaotic attractors generated by the Chua oscillator are taken into account. The two chaotic attractors correspond to two different sets of parameters. In the two experiments, the nonlinearity has the same qualitative form, but different parameters. The slopes of the two considered nonlinearities also differ for their sign, this leads to two different circuits constituting two interesting case studies.

From Eq. (1), the classical double scroll attractor shown by the Chua's circuit is obtained for the following parameters: $\delta=1$, $\alpha=9$, $\beta=14.286$, $\gamma=0$, $m_0=-1/7$, and $m_1=2/7$. The double scroll attractor shown by this circuit is reported

*mfrasca@diees.unict.it

†dcyu@uestc.edu.cn

‡lfortuna@diees.unict.it

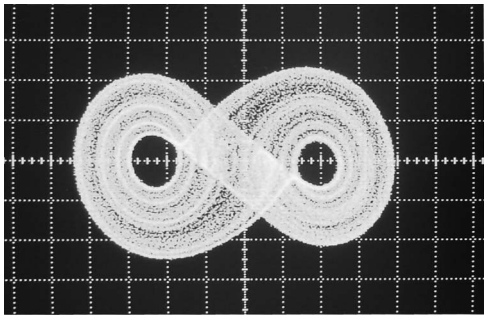

FIG. 1. Experimental results: projection on the x_2-x_3 plane of the double scroll attractor. Horizontal axis: 1 V/div; vertical axis 200 mV/div.

in Fig. 1. The second circuit is obtained for the following set of parameters: $\delta=-1$, $\alpha=-1.5601$, $\beta=0.0156$, $\gamma=0.1581$, $m_0=0.7562$, and $m_1=0.9575$. The experimental attractor obtained with these parameters is shown in Fig. 2.

II. THEORY

Let us consider a generic nonlinear system described by

$$\dot{\mathbf{x}} = \mathbf{f}(\mathbf{x}), \tag{2}$$

where $\mathbf{x}=[x_1,x_2,\ldots,x_n]^T \in \mathbb{R}^n$ represents the state vector and $\mathbf{f}=[f_1,f_2,\ldots,f_n]^T:\mathbb{R}^n \to \mathbb{R}^n$ is the dynamics of the system.

Let us then add to system (2) a control input of the following form:

$$\mathbf{u} = -\mathbf{k}(\mathbf{x}-\boldsymbol{\Theta}), \tag{3}$$

so that the controlled system reads

$$\dot{\mathbf{x}} = \mathbf{f}(\mathbf{x}) - \mathbf{k}(\mathbf{x}-\boldsymbol{\Theta}), \tag{4}$$

where the gain matrix $\mathbf{k}=\mathrm{diag}\{k_1,k_2,\ldots,k_n\}$ is a diagonal matrix with nonnegative elements k_i and $\boldsymbol{\Theta}=[\vartheta_1,\vartheta_2,\ldots,\vartheta_n]^T \in \mathbb{R}^n$ is a constant vector to be specified.

It has been shown [28] that if a proper gain matrix $\mathbf{k}$ is used, the system (4) can be driven to a steady state ($\dot{\mathbf{x}}=0$) satisfying,

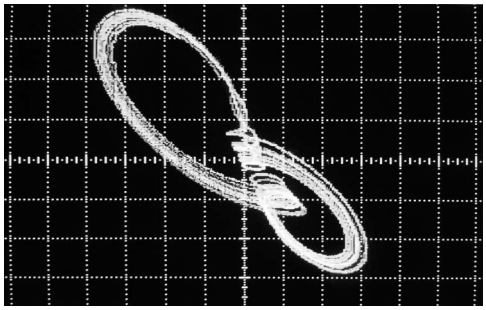

FIG. 2. Experimental results: projection on the x_2-x_3 plane of the chaotic attractor obtained by the Chua oscillator with parameters $\delta=-1$, $\alpha=-1.5601$, $\beta=0.0156$, $\gamma=0.1581$, $m_0=0.7562$, and $m_1=0.9575$. Horizontal axis: 2 V/div; vertical axis 200 mV/div.

$$\mathbf{f}(\mathbf{x}) = \mathbf{k}(\mathbf{x}-\boldsymbol{\Theta}). \tag{5}$$

To estimate the function $\mathbf{f}(\mathbf{x})$, one needs to apply Eq. (5) with m different values of the constant vector $\boldsymbol{\Theta}$. In this way m different data pairs $\{\mathbf{x}_m,\mathbf{k}(\mathbf{x}_m-\boldsymbol{\Theta}_m)\}$ can be obtained to represent the input-output relation of the function $\mathbf{f}$, from which the function $\mathbf{f}$ can be estimated. In particular, we will show a neural-network-based approach to estimate the function $\mathbf{f}$ from the obtained data pairs $\{\mathbf{x}_m,\mathbf{k}(\mathbf{x}_m-\boldsymbol{\Theta}_m)\}$. In fact, the Cybenko theorem [37] guarantees that a single hidden-layer feed-forward neural network is capable of approximating any continuous multivariate function to any desired degree of accuracy from the input-output data pairs.

Especially, if the system Eq. (4) is driven to a steady state under the control signal Eq. (3) with $k_j=0$ for all $j \neq i$ (that is, only the i-th equation is controlled), then one gets

$$f_i(\mathbf{x}) = k_i(x_i - \vartheta_i), \tag{6}$$

which can similarly be applied to uncover the structural information (or property) of the function f_i.

Above analysis has explicitly shown the basic principle of the control-based structure identification method. Here, we focus on its potential applications of physical interest.

A. System modeling

As a first potential application, the control-based structure identification method can be applied to system modeling. Actually, after the function $\mathbf{f}$ has been estimated with arbitrary accuracy by using neural network approximation techniques [37], the following equation:

$$\dot{\mathbf{y}} = \bar{\mathbf{f}}(\mathbf{y}), \tag{7}$$

can thus be considered as a model to represent system [Eq. (2)], where the function $\bar{\mathbf{f}}$ is an estimation of function $\mathbf{f}$. Therefore, one may analyze the dynamical behavior and properties, the estimation of the initial conditions, and the synthesis issues of system (2) using the model (7).

1. Analyzing the dynamical behavior of a system from its model

It is usually difficult to analyze the dynamical behavior of a nonlinear system (esp. chaotic system) because: (i) it is sensitive to initial conditions and system parameters; and (ii) one, in practice, often cannot change the initial conditions of a nonlinear system. However, one may change the initial conditions of the model very easily. As a result, one can numerically analyze the influence of the initial conditions on the attractor structure or phase trajectories.

2. Estimating initial conditions of a nonlinear system

Let us consider the system (2) with initial conditions $\mathbf{x}(0)=\mathbf{x}_0$, which actually reads

$$\dot{\mathbf{x}} = \mathbf{f}(\mathbf{x},\mathbf{x}_0), \tag{8}$$

and its model (7) with initial conditions $\mathbf{y}(0)=\mathbf{y}_0$, given by

$$\dot{\mathbf{y}} = \bar{\mathbf{f}}(\mathbf{y},\mathbf{y}_0). \tag{9}$$

If $\mathbf{x}_0=\mathbf{y}_0$, system (8) and its model (9) may synchronize identically with each other at least in the very beginning stage,

even when system (8) is chaotic, that is, $\|\mathbf{y}(t)-\mathbf{x}(t)\|<\epsilon$ for all $0<t<T_s$, with sufficiently small ϵ and proper T_s. Otherwise, both systems generally cannot synchronize identically with each other and the synchronization error E_s, simply defined by $\Sigma_{i=1}^{N}\|\mathbf{y}(iT)-\mathbf{x}(iT)\|$ with proper sampling interval T, is a function of the variable $\mathbf{y}_0-\mathbf{x}_0$ and $\mathbf{x}_0$ can roughly be estimated by searching the minimal value of E_s.

3. Synchronization between a system and its model

Let us now move to analyze synchronization between a system and its model through adding proper unidirectional and bidirectional couplings, and revisit system (2) and its model (7) as an illustrating example. We first treat the unidirectional coupling case and add the coupling term $-\Psi(\mathbf{y}-\mathbf{x})$ to the right hand side of Eq. (7), where $\Psi=\mathrm{diag}\{\psi_1,\psi_2,\ldots,\psi_n\}$ denotes the coupling strength vector. In this case, the error system reads,

$$\dot{\mathbf{e}}=\bar{\mathbf{f}}(\mathbf{e}+\mathbf{x})-\bar{\mathbf{f}}(\mathbf{x})+\bar{\mathbf{f}}(\mathbf{x})-\mathbf{f}(\mathbf{x})-\Psi\mathbf{e}, \tag{10}$$

where $\mathbf{e}=\mathbf{y}-\mathbf{x}$.

When the coupling strengths ψ_i increase gradually and are beyond a critical value, the error system Eq. (10) may run into a small neighborhood around the origin point, since $\bar{\mathbf{f}}(\mathbf{x})\approx\mathbf{f}(\mathbf{x})$ is satisfied for any $\mathbf{x}$. In particular, if the identical synchronization manifold holds through unidirectional couplings of partial state variables (i.e., $\psi_i=0$ holds for some i), then the remaining state variables of system (2) can be estimated by the model. In this case, the model can actually be taken as a state observer for system (2). The above analysis can be extended to the bidirectional coupling case. One may significantly declare that the model (7) is good if the identical synchronization between system (2) and the model (7) holds through adding proper unidirectional and bidirectional couplings.

B. Identification of some elements of interest

In some applications, one may know partial structure of the whole system as a preknowledge but the structure of some functional elements may be unknown. For example, for coupled systems given by

$$\dot{\mathbf{x}}_1=\mathbf{g}_1(\mathbf{x}_1)+\mathbf{h}_1(\mathbf{x}_1,\mathbf{x}_2), \tag{11}$$

$$\dot{\mathbf{x}}_2=\mathbf{g}_2(\mathbf{x}_2)+\mathbf{h}_2(\mathbf{x}_1,\mathbf{x}_2), \tag{12}$$

where $\mathbf{x}_1\in\mathbb{R}^n$ and $\mathbf{x}_2\in\mathbb{R}^n$ are state vectors of systems (11) and (12), respectively; $\mathbf{g}_1$ and $\mathbf{g}_2$ describe the node dynamics; $\mathbf{h}_1$ and $\mathbf{h}_2$ are coupling functions. It is reasonable to assume that the local dynamics of each system may be known exactly but the coupling functions are not. It is of interest to estimate functions $\mathbf{h}_1$ and $\mathbf{h}_2$. By the control-based method, one may obtain estimated $\mathbf{f}_1$ and $\mathbf{f}_2$, where $\mathbf{f}_1(\mathbf{x}_1,\mathbf{x}_2)=\mathbf{g}_1(\mathbf{x}_1)+\mathbf{h}_1(\mathbf{x}_1,\mathbf{x}_2)$ and $\mathbf{f}_2(\mathbf{x}_1,\mathbf{x}_2)=\mathbf{g}_2(\mathbf{x}_2)+\mathbf{h}_2(\mathbf{x}_1,\mathbf{x}_2)$. Then $\mathbf{h}_1$ and $\mathbf{h}_2$ can easily be estimated.

Many chaotic systems (including Lorenz system, Rössler system, and Chua's circuits) can be put in the form

$$\dot{\mathbf{x}}=\mathbf{A}\mathbf{x}+\mathbf{h}(\mathbf{x}), \tag{13}$$

where $\mathbf{A}$ is a constant matrix and the nonlinearity $\mathbf{h}(\mathbf{x})$ is the essential element that may determine the existence and properties of chaos. To analyze the dynamical properties of system (13), one first has to estimate function $\mathbf{h}$.

III. IDENTIFICATION OF THE CHUA OSCILLATOR DYNAMICS AND NONLINEARITY

We apply control (3) to the Chua oscillator (1) and propose a method to identify either the whole structure of the circuit or a part of it (i.e., its nonlinearity). In the first case, we only suppose that the order of the system is known and the state variables are measurable and controllable. In the second case, we suppose that only some important structural information needs to be identified (in this case the $i-v$ characteristics of the nonlinear elements).

The equations of the Chua oscillator with control (3) become,

$$\begin{aligned}\dot{x}_1&=\delta\alpha[x_2-h(x_1)]-k_1(x_1-\vartheta_1),\\ \dot{x}_2&=\delta(x_1-x_2+x_3)-k_2(x_2-\vartheta_2),\\ \dot{x}_3&=\delta(-\beta x_2-\gamma x_3)-k_3(x_3-\vartheta_3),\end{aligned} \tag{14}$$

where positive k_i are control gains and ϑ_i are constants to be specified. In the following the two cases are described more in detail.

A. Identification of the Chua oscillator dynamics

Let us first consider the case in which the whole structure of the circuit has to be identified. As it is the case of the implementation of the Chua oscillator under examination [33], all the state variables are assumed measurable.

We start from Eq. (14) and follow this algorithm:

(1) We apply the control and let $\mathbf{\Theta}=[\vartheta_1,\vartheta_2,\vartheta_3]^T$ vary so that we obtain m pairs: $(\mathbf{x}_i,\mathbf{\Theta_i})$.

(2) From Eq. (5) we calculate $\mathbf{f}(\mathbf{x})=\mathbf{k}(\mathbf{x}-\Theta_\mathbf{i})$, so that to obtain m pairs: $(\mathbf{x}_i,\mathbf{f}(\mathbf{x}_i))$.

(3) We can now apply an identification technique to develop a model fitting the data obtained at point 2 (i.e., pairs $(\mathbf{x}_i,\mathbf{f}(\mathbf{x}_i))$). In particular, we use an approach based on neural networks. In fact, the Cybenko theorem [37] guarantees that a single hidden-layer feed-forward neural network is capable of approximating any continuous multivariate function to any desired degree of accuracy.

The approach illustrated for the Chua oscillator can be easily adapted to any other continuous nonlinear system and is quite independent of the particular identification technique adopted. Other identification techniques can be used in step 3. The approach described provides a black box model of the chaotic dynamics and not a reconstruction of the attractor or the learning of the state variable trends.

B. Identification of the Chua oscillator nonlinearity

Let us now suppose that the only unknown part of the Chua oscillator dynamics is the nonlinearity $h(x)$. Moreover, let us suppose that k_i are such that steady-state control is effective. Let us focus on the first equation of Eq. (14) and set $\dot{x}_1=0$ to obtain,

$$h(x_1) = x_2 - \frac{k_1(x_1 - \vartheta_1)}{\delta\alpha}. \quad (15)$$

Fixed ϑ_1, ϑ_2, and ϑ_3, Eq. (15) gives us a value for $h(x_1)$. By varying ϑ_1, ϑ_2, and ϑ_3 we can have a set of measures for $h(x_1(\vartheta_1, \vartheta_2, \vartheta_3))$ and use them to identify the nonlinearity appearing in the circuit.

In our case, it can be demonstrated that varying just one parameter $\vartheta \triangleq \vartheta_1$ is enough to have a complete set of measures to identify the nonlinearity $h(x_1)$, since the steady-state value of variable x_2 is a function of that of x_1. In practice, we kept constant ϑ_2 and ϑ_3 (to the values $\vartheta_2=0$ and $\vartheta_3=0$). In Sec. IV, we compare the ideal form of $h(\vartheta)$ with experimental data.

IV. EXPERIMENTAL RESULTS

A. Description of the experimental setup

The Chua's circuit (and its generalization known as the Chua oscillator) is one of the most studied third-order circuits able to show a large variety of chaotic attractors and bifurcation phenomena. During the years, many different implementations of the original circuit and, in particular, of its nonlinear element, the Chua's diode, have been introduced [33]. Among such possible implementations of the Chua oscillator the one based on Cellular Nonlinear Networks (CNN) (i.e., the so-called CNN-based implementation) has been chosen in our experiments. We will not describe in details this implementation, accurately dealt with in [33], but we briefly discuss the motivation for this choice and show the complete circuit diagram (including the modification for the introduction of the steady-state control).

In the CNN-based implementation of the Chua oscillator [33,38,39] all the physical variables implementing the state variables of Eq. (1) are voltages across capacitors (in particular, x_1 is the voltage across C_1, x_2 across C_2 and x_3 across C_3). The circuit makes use of properly configured operational amplifiers for implementing the mathematical operations appearing in Eq. (1). Furthermore, it exploits the saturation nonlinearity of an operational amplifier to implement the piecewise nonlinearity $h(x)$.

Since in this implementation, the state variables are easily accessible, the steady-state control in Eq. (4) can be easily implemented. In practice, the generic feedback term $-k(x-\Theta)$ of Eq. (14) (with $x=\{x_1,x_2,x_3\}$ and $\Theta=\{\vartheta_1,\vartheta_2,\vartheta_3\}$) is implemented by introducing a further operational amplifier in the circuit with two inputs, i.e., the state variable x and the reference voltage Θ. The gain of such generic block shown in Fig. 3 is given by $g=-\frac{R_f}{R_d}$ and is chosen so that $\frac{R_f}{R_d}=k$.

We used two Chua oscillators with different parameters, the first circuit is the classical Chua's circuit exhibiting the double scroll Chua's attractor where the implementation described in [38] is adopted; the second is a Chua oscillator designed to implement another chaotic attractor and developed following the guidelines discussed in [33]. In particular, we discuss the results of the application of the method to identify the whole dynamics to the classical Chua's circuit and, then, describe the case of the identification of the nonlinear elements for the two circuits. In fact, both have qualitatively the same nonlinearity (i.e., a piecewise linear function), but the slopes m_0 and m_1 of their nonlinearities are not equal and, in particular, have different signs. This along with the different sign of the parameters δ and α lead to two different case studies. The two circuits (including the control) are shown in Figs. 4 and 5.

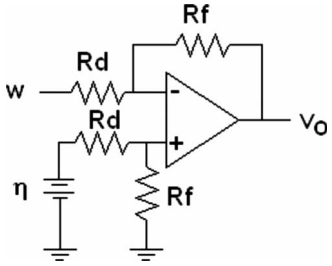

FIG. 3. Generic block used to implement the steady-state control.

In the first circuit the control is represented by operational amplifiers $U5$-$U7$, while the rest of the circuit is the CNN-based implementation of the Chua's circuit. The parameters of this part of the circuit have been chosen according to [38]: $R_1=3.9$ kΩ, $R_2=12$ kΩ, $R_3=5.6$ kΩ, $R_4=22$ kΩ, $R_5=22$ kΩ, $R_6=450$ Ω, $R_7=100$ kΩ, $R_8=100$ kΩ, $R_9=100$ kΩ, $R_{10}=100$ kΩ, $R_{11}=100$ kΩ, $R_{12}=1$ kΩ, $R_{13}=8.2$ kΩ, $R_{14}=100$ kΩ, $R_{15}=8.2$ kΩ, $R_{16}=100$ kΩ, $R_{17}=1$ kΩ, $R_{18}=82$ kΩ, $R_{19}=82$ kΩ, $R_{20}=1000$ kΩ, $R_{21}=1000$ kΩ, $R_{22}=12.1$ kΩ, $R_{23}=1$ kΩ, $C_1=100$ nF, $C_2=100$ nF, and $C_3=100$ nF.

The parameters of the part of the circuit implementing the steady-state control have been chosen to set the control gain to $k_1=3$ and $k_2=k_3=1$: $R_{24}=300$ kΩ, $R_{25}=100$ kΩ, $R_{26}=100$ kΩ, $R_{27}=300$ kΩ, $R_{28}=100$ kΩ, $R_{29}=100$ kΩ, $R_{30}=50$ kΩ, $R_{31}=100$ kΩ, $R_{32}=100$ kΩ, $R_{33}=50$ kΩ, $R_{34}=22$ kΩ, $R_{35}=100$ kΩ, and $R_{36}=100$ kΩ. TL084 have been used as operational amplifiers.

Without control the circuit generates the double scroll Chua's attractor shown in Fig. 1. When control is activated, the circuit is controlled to a steady-state constant behavior (stable fixed equilibrium point) whose value depends on $\boldsymbol{\Theta}$.

In the second circuit the control is represented by operational amplifiers $U6$-$U8$, while the rest of the circuit implements the Chua oscillator. The parameters of this part of the circuit have been chosen according to [38]: $R_1=22$ kΩ, $R_2=11.2$ kΩ, $R_3=22$ kΩ, $R_4=23.3$ kΩ, $R_5=23$ kΩ, $R_6=670$ kΩ, $R_7=100$ kΩ, $R_8=100$ kΩ, $R_9=50$ kΩ, $R_{10}=100$ kΩ, $R_{11}=100$ kΩ, $R_{12}=1$ kΩ, $R_{13}=630$ kΩ, $R_{14}=84.6$ kΩ, $R_{15}=23.5$ kΩ, $R_{16}=100$ kΩ, $R_{17}=22$ kΩ, $R_{18}=1$ kΩ, $R_{19}=1000$ kΩ, $R_{20}=75$ kΩ, $R_{21}=75$ kΩ, $R_{22}=12.1$ kΩ, $R_{23}=1$ kΩ, $R_{24}=1000$ kΩ, $R_{26}=500$ kΩ, $R_{27}=15.5$ kΩ, $R_{28}=50$ kΩ, $R_{29}=22$ kΩ, $C_1=100$ nF, $C_2=100$ nF, and $C_3=100$ nF.

The parameters of the part of the circuit implementing the steady-state control have been chosen to set the control gain to $k_1=k_2=k_3=5$: $R_{30}=20$ kΩ, $R_{31}=20$ kΩ, $R_{32}=100$ kΩ, $R_{33}=100$ kΩ, $R_{34}=100$ kΩ, $R_{35}=100$ kΩ, $R_{36}=20$ kΩ, $R_{37}=20$ kΩ, $R_{38}=16.6$ kΩ, $R_{39}=16.6$ kΩ, $R_{40}=23$ kΩ, $R_{41}=100$ kΩ, $R_{42}=100$ kΩ, $R_{43}=23$ kΩ, $R_{44}=100$ kΩ,

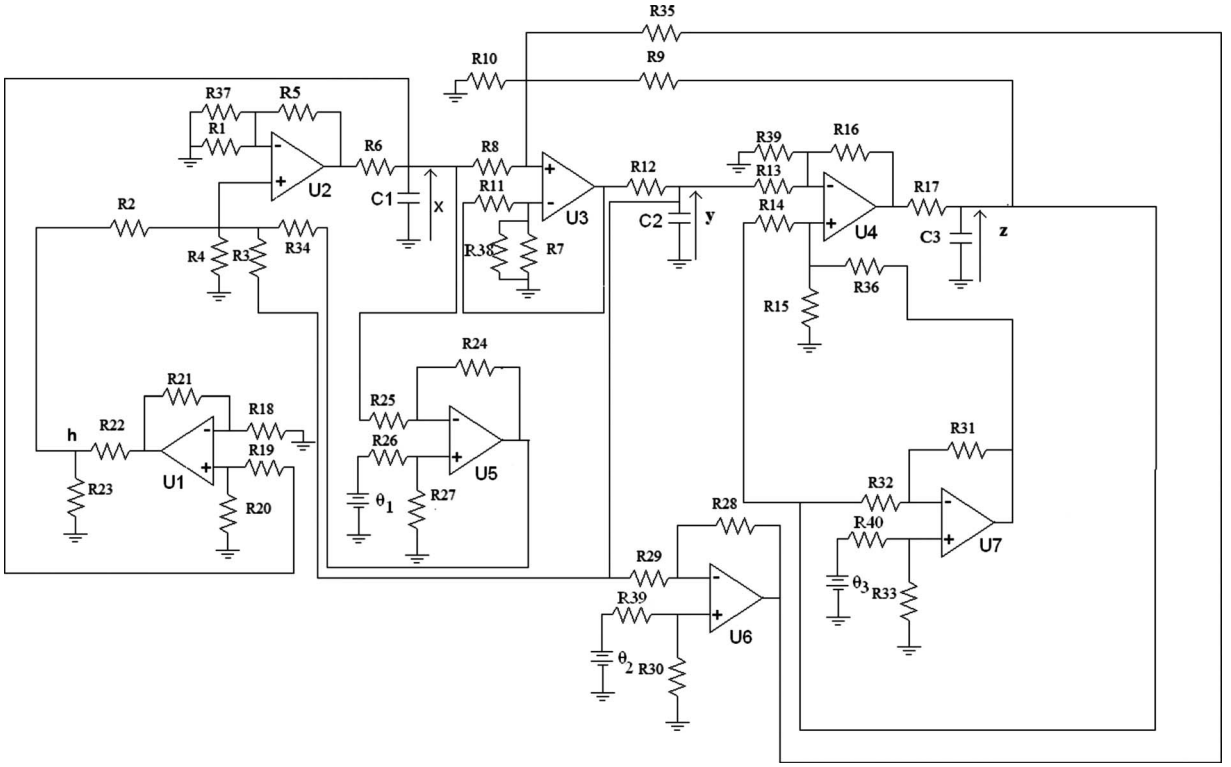

FIG. 4. The Chua oscillator (including the control circuitry) generating the double scroll strange attractor shown in Fig. 1.

and $R_{45}=100$ kΩ. TL084 have been used as operational amplifiers.

Without control the circuit generates the chaotic attractor shown in Fig. 2. When control is activated, the circuit is controlled to a steady-state constant behavior (stable fixed equilibrium point) whose value depends on **Θ**.

The whole experimental setup consists of the Chua oscillator, a voltage power supply, voltage generators used to vary **Θ**, and an acquisition board (National Instruments AT-MIO 1620E) used to acquire the data.

B. Identification of the whole dynamics

Let us first discuss the experimental results related to the identification of the whole dynamics of the classical Chua's circuit (shown in Fig. 4). We fixed **Θ**, waited that the circuit

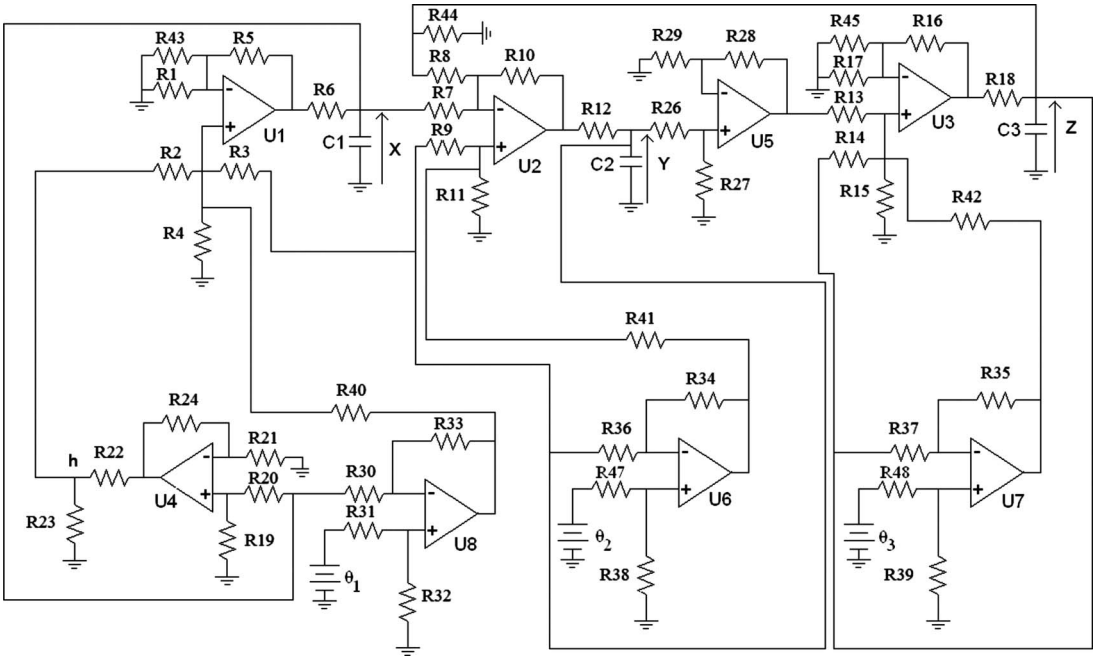

FIG. 5. The Chua oscillator (including the control circuitry) generating the strange attractor shown in Fig. 2.

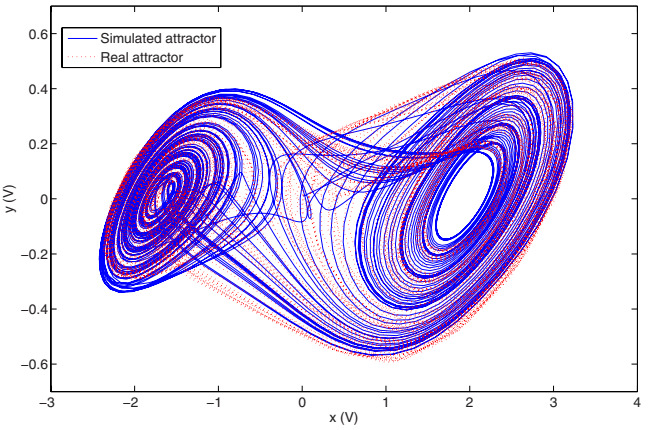

FIG. 6. (Color online). Experimental results: comparison between a real double scroll strange attractor and the attractor generated by the neural network model.

reached the steady-state and then acquired $\bar{\mathbf{x}}$. From Eq. (5) the corresponding value of $\mathbf{f}(\mathbf{x})$ was then derived. The process was repeated N times. More in detail, we used $11\times11\times11$ (i.e., $N=1331$) pairs of data $(\mathbf{x}_i,\mathbf{f}(\mathbf{x}_i))$.

A neural network with 18 hidden neurons was then trained for 3000 epochs. The data were divided in 50% as training set, 25% as validation set, and 25% as test set. The neural network model was then compared with the real data as shown in Fig. 6. Due to the sensitivity of chaotic systems to initial conditions the trajectories of the model and of the real system diverge, but the structure in the phase plane (i.e., the attractor) is clearly the same.

C. Estimation of the initial conditions

As a possible application of our approach, we studied the problem of estimating the initial conditions of the Chua oscillator. We assumed that only one circuit state variable (namely the variable x_1) is available (it can be demonstrated [40] that linear feedback control on this state variable is sufficient to stabilize a fixed equilibrium point in the Chua oscillator dynamics). We then simulated the neural network model for a time interval 0.8 s (which is sufficiently long if compared to the characteristic frequencies of the circuit having maximum frequency in the order of magnitude of some kilohertz) and searched for that part of such trajectory minimizing the synchronization error defined on the basis of the only information available: $E_s=\Sigma_{i=1}^{N}|y_1(iT)-x_1(iT)|$. We fixed $T_s=3$ ms (which, given a sampling rate of $f=50$ kHz corresponds to $N=150$ samples). The initial conditions of the model are used to estimate the real ones. Following this approach, we obtained $y_1(0)=1.3069$, $y_2(0)=0.2083$, and $y_3(0)=-0.5055$, which provide a good estimation of the real initial conditions of the circuit: $x_1(0)=1.2830$, $x_2(0)=0.1870$, and $x_3(0)=-0.4710$. Figure 7 shows the comparison between the trend of the model state variables and that of the circuit state variables. The accuracy of the initial conditions estimation can be increased by taking into account a longer simulation time interval at the expenses of increasing computational efforts. However, due to sensitiveness of chaotic systems to initial conditions, the obtained accuracy is satisfying for the purpose, i.e., to provide insight on working conditions of the real system, eventually in the perspective of short-term prediction.

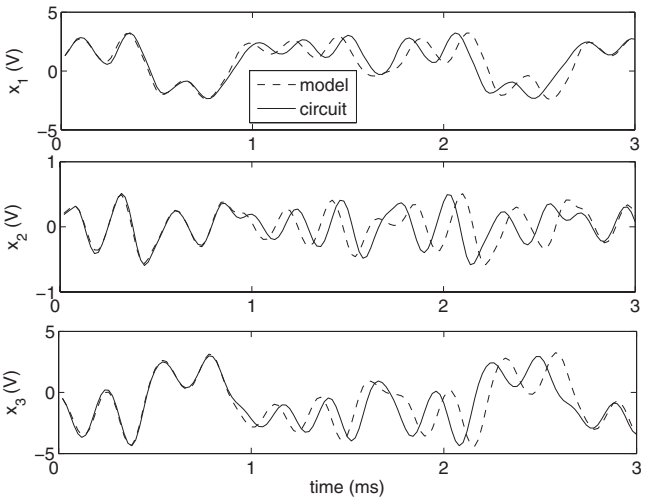

FIG. 7. Estimation of the circuit initial conditions: comparison between the trend of the model state variables and that of the circuit state variables.

D. Synchronization between the Chua oscillator and its model

As discussed in Sec. II the model derived through the steady-state control method can be validated by studying if adding unidirectional or bidirectional coupling it can be synchronized with the nominal model of the system. In fact, in our case, the nominal model of the circuit can be easily derived, since the equations of the Chua oscillator are known and the parameters really implemented in the circuit can be accurately measured. The need for such preliminary operation (to derive the circuit model) is further motivated in the next Section, showing how the nominal parameters of Eq. (1) cannot be used in a realistic model.

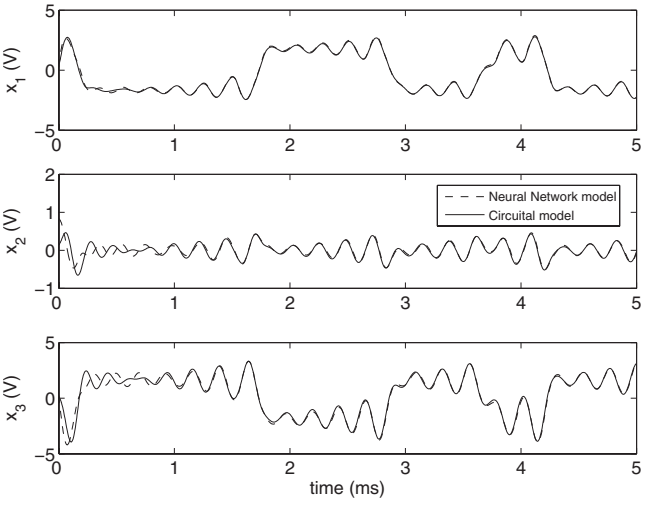

FIG. 8. Synchronization between the neural network model and the nominal model of the Chua oscillator: trend of the state variables of the two models.

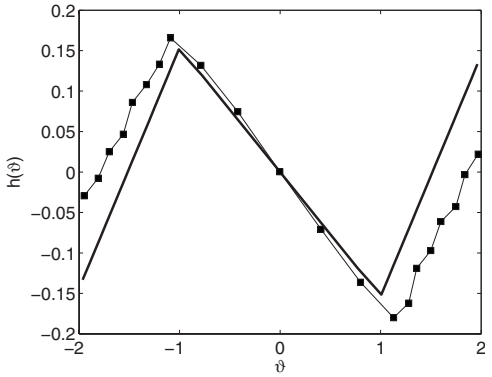

FIG. 9. Experimental results: characterization of the nonlinearity appearing in the first circuit.

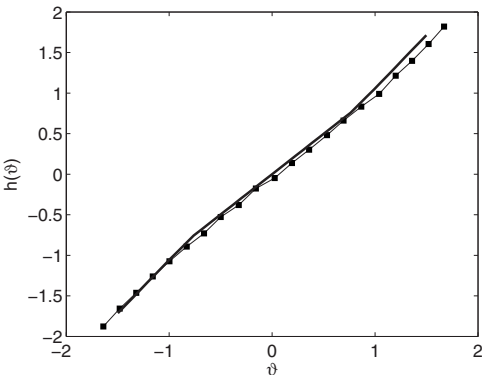

FIG. 10. Experimental results: characterization of the nonlinearity appearing in the second circuit.

Figure 8 shows the results of a simulation in which the neural network model is bidirectionally coupled (through the state variable x_1) to the nominal model of the Chua oscillator. As the obtained results clearly demonstrate, the synchronization error $e(t)$ is close to zero (after the transient, $|e(t)| < 0.15$ V) and identical synchronization holds.

E. Identification of the nonlinear elements

Let us now focus on the possibility of using the approach based on steady-state control to identify some important part of the system (such as coupling or nonlinear elements), known the remaining part of the dynamics. In particular, let us suppose that the nonlinearity of the Chua oscillator has to be identified. Without any lack of generality we set: $\vartheta_2=0$, $\vartheta_3=0$, and $\vartheta \triangleq \vartheta_1$.

Experimental results have been obtained by varying ϑ, acquiring $x_1(\vartheta)$, $x_2(\vartheta)$, and $x_3(\vartheta)$ and then applying Eq. (15) to calculate the estimated nonlinearity.

Figures 9 and 10 show the comparison between the measured nonlinearity and the ideal one for the two circuits. In both figures the continuous line represents the ideal (simulated) curve, while squares represent experimental data. From the analysis of Fig. 9 it can be derived that the breakpoints of the nonlinearity are not accurately implemented in our circuit, and the real values are slightly larger than the ideal ones. The presence of such error has no particular consequences since the double scroll Chua's attractor is robust to small parameter variations and, in fact, the implemented circuit makes use of off-the-shelf resistors with 5% tolerance. *A posteriori* we have effectively verified that the resistances implementing the breakpoint parameters do not have very precise values.

The same consideration does not apply to the second chaotic attractor, which is quite sensitive to parameter changes. The circuit exhibiting this attractor has been implemented by using off-the-shelf resistors with 1% tolerance. The analysis of Fig. 10 reveals that data fit quite well the ideal nonlinearity.

We remark that, since linear feedback control on the state variable x_1 is sufficient to stabilize a fixed equilibrium point in the Chua's circuit dynamics [40] and $\theta_2=\theta_3=0$ in all the identification process of the nonlinearity, $h(x_1)$ can be also identified by controlling only the first state variable.

V. CONCLUSIONS

We have shown that driving a system to steady states is an effective method for the identification of the dynamics of a nonlinear system (e.g., chaotic circuit). The method consisting of the introduction of a feedback control input in the complex system has proved, under the hypotheses of measurable state variables and physical access to the system for implementing the proportional feedback, to be effective in the estimation of attractor structure, initial conditions, state variables, or structure of some elements of interest. In this work, we have experimentally verified the suitability of the method by taking into account the problem of estimating initial conditions of a chaotic circuit and identifying the dynamics of a chaotic circuit or some important part of it (such as the nonlinearity). In particular, two different cases (two attractors of the Chua oscillator) have been examined. The experimental results shown in the paper demonstrate the suitability of the method in real hardware experiments, despite the presence of noise and parameter tolerances.

ACKNOWLEDGMENTS

This work was partially supported by the National Natural Science Foundation of China under Grant Nos. 106020206 and 60934002.

[1] U. Parlitz, Phys. Rev. Lett. **76**, 1232 (1996).
[2] D. Yu and U. Parlitz, Phys. Rev. E **77**, 066221 (2008).
[3] D. Yu and F. Liu, Chaos **18**, 043108 (2008).
[4] D. Yu and A. Wu, Phys. Rev. Lett. **94**, 219401 (2005).
[5] A. Maybhate and R. E. Amritkar, Phys. Rev. E **61**, 6461 (2000).
[6] R. Konnur, Phys. Rev. E **67**, 027204 (2003).
[7] C. Tao, Y. Zhang, G. Du, and J. J. Jiang, Phys. Rev. E **69**, 036204 (2004).
[8] U. S. Freitas, E. E. N. Macau, and C. Grebogi, Phys. Rev. E **71**, 047203 (2005).
[9] I. P. Marino and J. Miguez, Phys. Rev. E **72**, 057202 (2005).
[10] D. B. Huang, Phys. Rev. E **69**, 067201 (2004).
[11] D. Huang and R. Guo, Chaos **14**, 152 (2004).
[12] J. Lu and J. Cao, Chaos **15**, 043901 (2005).
[13] H. Fujisaka and T. Yamada, Prog. Theor. Phys. **69**, 32 (1983).
[14] L. M. Pecora and T. L. Carroll, Phys. Rev. Lett. **64**, 821 (1990).
[15] S. Boccaletti, J. Kurths, G. Osipov, D. L. Valladares, and C. Zhou, Phys. Rep. **366**, 1 (2002).
[16] D. Creveling, J. Jeanne, and H. D. I. Abarbanel, Phys. Lett. A **372**, 2043 (2008).
[17] H. D. I. Abarbanel, D. R. Creveling, and J. M. Jeanne, Phys. Rev. E **77**, 016208 (2008).
[18] D. Yu and U. Parlitz, Phys. Rev. E **77**, 066208 (2008).
[19] R. Femat and G. Solis-Perales, Phys. Rev. E **65**, 036226 (2002).
[20] U. Parlitz, L. Junge, and L. Kocarev, Phys. Rev. E **54**, 6253 (1996).
[21] E. Baake, M. Baake, H. G. Bock, and K. M. Briggs, Phys. Rev. A **45**, 5524 (1992).
[22] H. U. Voss, J. Timmer, and J. Kurths, Int. J. Bifurcation Chaos Appl. Sci. Eng. **14**, 1905 (2004).
[23] D. R. Creveling, P. E. Gill, and H. D. I. Abarbanel, Phys. Lett. A **372**, 2640 (2008).
[24] J. Bröcker, U. Parlitz, and M. Ogorzalek, Proc. IEEE **90**, 898 (2002).
[25] R. Hegger, M. J. Bünner, H. Kantz, and A. Giaquinta, Phys. Rev. Lett. **81**, 558 (1998).
[26] M. Siefert, Phys. Rev. E **76**, 026215 (2007).
[27] V. I. Ponomarenko and M. D. Prokhorov, Phys. Rev. E **78**, 066207 (2008).
[28] D. Yu and F. Liu, Phys. Rev. E **78**, 017201 (2008).
[29] D. Yu and U. Parlitz, Europhys. Lett. **81**, 48007 (2008).
[30] D. Yu, L. Fortuna, and F. Liu, Chaos **18**, 043101 (2008).
[31] D. Yu, M. Frasca, and F. Liu, Phys. Rev. E **78**, 046209 (2008).
[32] D. Yu and S. Boccaletti, Phys. Rev. E **80**, 036203 (2009).
[33] L. Fortuna, M. Frasca, and M. G. Xibilia, *Chua's Circuit Implementations: Yesterday, Today and Tomorrow* (World Scientific, Singapore, 2009).
[34] L. O. Chua, M. Komuro, and T. Matsumoto, IEEE Trans. Circuits Syst., I: Regul. Pap. **33**, 1073 (1986).
[35] L. O. Chua and G.-N. Lin, IEEE Trans. Circuits Syst., I: Regul. Pap. **37**, 885 (1990).
[36] R. Madan, *Chua's Circuit: A Paradigm for Chaos* (World Scientific, Singapore, 1993).
[37] G. V. Cybenko, Math. Control, Signals, Syst. **2**, 303 (1989).
[38] P. Arena, S. Baglio, L. Fortuna, and G. Manganaro, IEEE Trans. Circuits Syst., I: Regul. Pap. **42**, 123 (1995).
[39] P. Arena, S. Baglio, L. Fortuna, and G. Manganaro, IEICE Trans. Fundamentals **79-A**, 1647 (1996).
[40] G. Chen, IEEE Trans. Circuits Syst., I: Regul. Pap. **40**, 829 (1993).